

## Toward quantitative bremsstrahlung medical imaging by custom gamma camera device

Capogni, Marco; Cisbani, Evaristo; Cosmi, Valerio; Croia, Michele; Giuliani, Fausto; Limiti, Giulia; Lucentini, Maurizio; Murri, Silvio; Musico, Paolo; More Authors

**DOI**

[10.1051/epjconf/202533809005](https://doi.org/10.1051/epjconf/202533809005)

**Publication date**

2025

**Document Version**

Final published version

**Published in**

EPJ Web of Conferences

**Citation (APA)**

Capogni, M., Cisbani, E., Cosmi, V., Croia, M., Giuliani, F., Limiti, G., Lucentini, M., Murri, S., Musico, P., & More Authors (2025). Toward quantitative bremsstrahlung medical imaging by custom gamma camera device. *EPJ Web of Conferences*, 338, Article 09005. <https://doi.org/10.1051/epjconf/202533809005>

**Important note**

To cite this publication, please use the final published version (if applicable).  
Please check the document version above.

**Copyright**

Other than for strictly personal use, it is not permitted to download, forward or distribute the text or part of it, without the consent of the author(s) and/or copyright holder(s), unless the work is under an open content license such as Creative Commons.

**Takedown policy**

Please contact us and provide details if you believe this document breaches copyrights.  
We will remove access to the work immediately and investigate your claim.

# Toward quantitative bremsstrahlung medical imaging by custom gamma camera device

Marco Capogni<sup>1</sup>, Evaristo Cisbani<sup>2,\*</sup>, Valerio Cosmi<sup>3</sup>, Michele Croia<sup>4</sup>, Fausto Giuliani<sup>2</sup>, Giulia Limiti<sup>5</sup>,  
Maurizio Lucentini<sup>2</sup>, Silvio Murri<sup>6</sup>, Paolo Musico<sup>7</sup>, Maurizio Pilade<sup>8</sup>, Fabio Santavenere<sup>2</sup>, Alessandro Spurio<sup>2</sup>

<sup>1</sup>Istituto Nazionale di Metrologia delle Radiazioni Ionizzanti (INMRI), ENEA Casaccia R.C., (Rome), Italy

<sup>2</sup>Istituto Superiore di Sanità, Rome, Italy

<sup>3</sup>Technische Universiteit Delft, Delft, The Netherlands

<sup>4</sup>Nuclear Research Reactors Laboratory, ENEA Casaccia R.C., (Rome), Italy

<sup>5</sup>STMicroelectronics, Cornaredo, Milan, Italy

<sup>6</sup>Azienda Ospedaliera-Universitaria Sant'Andrea, UOD Fisica Sanitaria, Rome, Italy

<sup>7</sup>Istituto Nazionale di Fisica Nucleare, Sezione di Genova, Genoa, Italy

<sup>8</sup>Sapienza University of Rome, Rome, Italy

(\* ) evaristo.cisbani@iss.it

**Abstract** — Bremsstrahlung radiation imaging may play an important role in the quantitative evaluation of the spatial-temporal distribution of the  $\beta^-$  radioactive emitters in order to optimize and personalize the methodology and dosage of radiopharmaceuticals in radiometabolic therapy.

The present work is an attempt to investigate quantitative bremsstrahlung imaging aspects, using a configurable phantom based experimental apparatus with corresponding simulated model, to highlight critical issues and pitfalls, and to identify, whenever possible, directions to overcome, mitigate or likely take advantage of some of them. Procedure for precise phantom activity determination by portable counter, Monte Carlo fine tuning, definition of figures of merit for the choice of optimal image reconstruction parameters, and correction factors for the activity estimation are some of the main explored details to end up with a preliminary quantitative imaging obtained by simulation-measurement comparison.

**Keywords** — Radiometabolic therapy, Quantitative Imaging.

## I. INTRODUCTION

THE specificity of radiometabolic therapy and the potential of a personalized approach make this treatment one of the most promising therapeutic protocol in clinical precision medicine. In fact, radiometabolic therapy is a clinical treatment that involves the administration of specific radiopharmaceutical to kill and prevent further development of cancer cells by targeting them at molecular level [1]. Its effectiveness depends on maximizing radiation damage to the tumor region while minimizing its potential toxicity to healthy organs and tissues. This is achieved by enhancing the uptake of the radiopharmaceutical by tumor cells and therefore selecting the most appropriate pharmaceutical ligands combined with radio isotopes emitting short-range, high energy transfer particles which provide highly biological effectiveness in the tumor region.

The quantitative determination of the spatial and temporal

bio-distributions of the administered therapeutic agent, which possesses patient specific characteristics, is a crucial aspect of personalized optimization of the radioisotope dosage; this is essential both for assessing therapy effectiveness and for verifying the actual administered dose during treatment. The necessary information can be obtained non-invasively, possibly in combination with blood tests or other clinical analyses, by imaging the radiation emitted by the therapeutic radioactive substance, which can escape from the patient's body. Quantitative analysis of these images permits the estimation of distribution of the radiopharmaceutical isotope activities in each region of interest. The time dependent activity can then be related to relevant radiobiological quantities, *in primis* the absorbed dose.

Performing quantitative imaging in radiometabolic therapy is generally challenging due to different factors, including the peculiarities of involved radionuclides. Moreover, defining and quantifying the volumes of interest are also critical: images in nuclear medicine are functional-based, so the volumes identified from these images do not necessarily correspond to anatomical volumes, which are instead reconstructed in Computed Tomography (CT) or Magnetic Resonance Imaging (MRI).

In this context, the Bremsstrahlung radiation imaging technique may play an important role for radiopharmaceuticals with (almost) pure  $\beta^-$  (and  $\beta^+$ ) emitters, such as yttrium-90 (<sup>90</sup>Y), used in radiometabolic therapy. While electrons perform their therapeutic task by releasing most of their energy to cells close to the point of radionuclide decay, the bremsstrahlung gamma radiation emitted from the same electrons can escape from the patient and be detected. However, this indirect radiation makes imaging quite complex, especially when administered radiopharmaceutical distribution shall be quantified. In fact, despite initial attempts at quantitative bremsstrahlung imaging dating back to 1980s and improvements on image reconstruction are progressing, clinical exploitation is still at the research level and not yet routinely adopted.

Therefore, the main aim of the proposed work has been the setup of an experimental apparatus and methodology to investigate quantitative bremsstrahlung imaging aspects, in order to highlight critical issues and pitfalls. Compared to most of the previous works in this field, we are considering relatively simplified, but as much as possible controlled experimental conditions: well-known emitter activities ( $^{90}\text{Y}$ ), custom gamma camera including readout electronics and reconstruction algorithms; we also minimized attenuation and scattering effects by adopting, in the initial phase, simple, small phantoms. This approach should help to better disentangle physics and reconstruction effects that contribute to the bremsstrahlung quantitative imaging, allowing for a more straightforward analysis of potential sources of image degradation and identifying potential improvements. The data acquired on real measurements have been complemented by detailed Monte Carlo (MC) simulations and corresponding data analysis, which are then used to produce quantitative assessment but also better evaluate the overall imaging process.

## II. EXPERIMENTAL APPROACH

The initial experimental apparatus used to study the quantitative bremsstrahlung radiation imaging (QBSI) aspects is characterized by the following main components:

- Radionuclide: weighted solution of yttrium-90 Dichloride ( $^{90}\text{YCl}_2$ )
- Portable TDCR (Triple-to-Double Coincidence Ratio) counter [2] for direct and precise on site activity measurement of the radioactive solution and related samples.
- Phantoms: two simple polymethyl methacrylate (PMMA) cylinders, 40 and 60 mm diameters, 13.9 and 19.7 mm heights, with 3 cylindrical cavities each filled by different  $^{90}\text{Y}$  solutions, in the bottom side and a PMMA lid on top.
- Detector consists of a compact, custom gamma camera based on two detection heads with complementary collimators and sizes. The small head includes a pin hole tungsten collimator with 1.2 mm hole diameter, 2 mm thickness, an NaI(Tl) pixelated scintillator with 2 mm pitch,  $50 \times 50 \text{ mm}^2$  active area and 5 mm thickness, optically coupled to a single Hamamatsu H8500 photomultiplier. The other larger detection head is equipped by a 20 mm thick,  $150 \times 200 \text{ mm}^2$  active area defined by a parallel hexagonal holes lead collimator with 2.1 mm pitch and 0.3 mm septa, a pixelated NaI(Tl) scintillator 1.5 mm pitch, 6 mm thickness coupled to a  $3 \times 4$  matrix of H8500 photomultipliers. At the time of measurement, this detector, originally designed for diagnostic scintigraphy research [3], was characterized and calibrated but not fully optimized for QBSI. Figure 1 shows a representative experimental setup with detectors and phantoms. The 832 photomultiplier

pixels are readout by modular electronics based on the MAROC3 front-end ASIC, which allow single channel signal shaping, with configurable self-triggering capabilities [4].

- Monte Carlo simulator is based on OpenGate/Geant4 toolkit [5] used to identify optimal reconstruction methods and provide normalization factors for quantitative imaging of the activities evaluation. Figure 2 show an example of simulated model. For the simulation of the physics processes involved into the detector as a consequence of the  $^{90}\text{Y}$  decay, the Penelope physics library (G4EmPenelopePhysics) has been adopted which should be preferred in the low energy region, and up to several MeV, for the simulation of the bremsstrahlung processes, compared to Livermore (G4EmLivermorePhysics) and Standard Physics (G4EmStandardPhysics) [6].

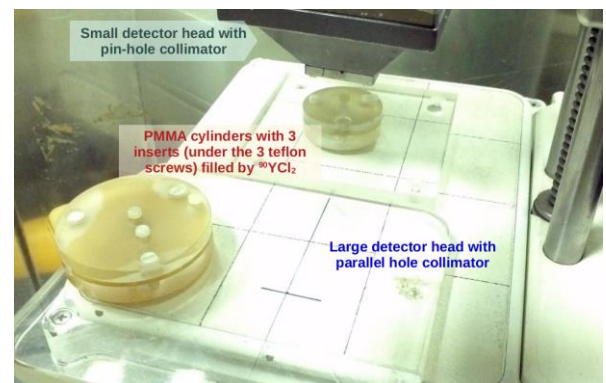


Fig. 1. Typical experimental configuration with the two phantoms on top of the large detector entrance window.  $^{90}\text{YCl}_2$  liquid solution is deposited in the cavities under the three small Teflon screws in each PMMA phantom disk; on the upper side visible the pin-hole collimator of the small head.

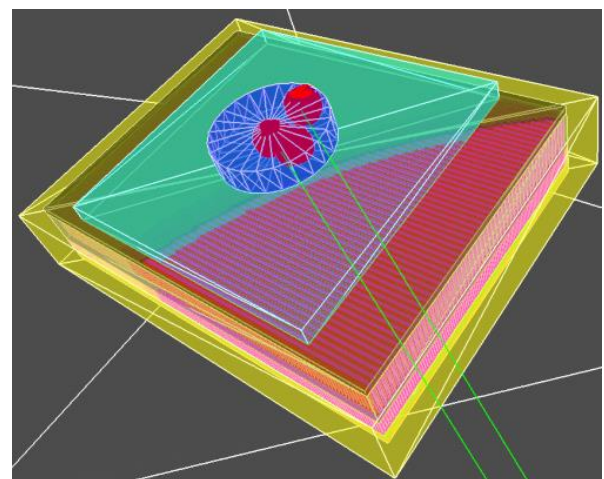


Fig. 2. Example of simulated model, with large phantom (in blue) and the three inserts with  $^{90}\text{YCl}_2$  radioactive liquid (red) resting on a plate of PMMA (green) above the detector; in yellow the detector Pb external case. Note: inserts appear larger than they are simulated for a rendering of the graphics engine used.

Acquisitions of the two phantoms radiation with different amounts of  $^{90}\text{YCl}_2$  on the inserts have been carried on using the dual head detectors and the corresponding setup modeled by the MC. The quantity of  $^{90}\text{YCl}_2$  liquids in each insert (from

about 1.0 to 2.1 MBq) has been estimated combining the portable TDCR activity measurement (accuracy of 1 kBq) of the liquid before filling the inserts and the weights (0.1 mg accuracy) of the phantom after each insert filling.

### III. DATA PROCESSING AND ANALYSIS

The image reconstruction from MC data offers the possibility to evaluate the effects of energy and hit cluster cuts, insert and background mask regions, and eventually determine the optimal trade-off.

Three indices have been defined to quantify the quality of the MC image reconstruction and therefore fine tune the energy window for the real data: the positional residue, the signal intensity and the noise level. The positional residue, a measure of spatial resolution, is the distance between the reconstructed hit position and the position of the  $^{90}\text{Y}$  that generated the interacting particle (ground truth) projected on the sensor plane and normalized by the number of hits in the event. The signal intensity is the sum of intensities of those hits that have a positional residue below a certain threshold, which in the present analysis has been set to 2.1 mm, that is 3 times the expected resolution of the detector ( $\sigma=0.7$  mm). The noise level is the complement of the signal intensity, that is the sum of intensities of those hits that have a positional residual larger than the 2.1 mm threshold.

Ideally the optimal setting corresponds to the maximum signal intensity and minimum positional residue and noise level; however these conditions do not occur for the same setting and therefore the overall optimization function shall be a weighted combination of the three conditions; the choice of such function is still under investigation and it somehow depends, in a clinical environment, on the final task of the image utilization. In the present preliminary analysis, the signal intensity over the noise level (signal to noise ratio) has been maximized ending up with the 30 to 266 keV energy interval, corresponding to the bottom image in fig 3 where different energy cuts are applied to a typical simulation of the large phantom detected by the parallel-hole sensor head; as expected, the energy cuts have the larger impact; the choice of these cuts are mainly driven by the adopted collimator, that in the present work consists in the medium energy, diagnostic optimized, parallel hole described above.

The responses of the more than 700 anodes that make up the light sensors coupled to the scintillators should be, ideally, statistically identical when the detector is subjected to a spatially uniform irradiation (flood). For realizing this condition, the acquisition electronics allows to assign to each anode channel a gain (from 0 to 4, with 256 steps), which helps to equalize the response of the anodes during acquisition, which is critical for effective self-trigger logic (AND of at least 3 channels) during acquisition.

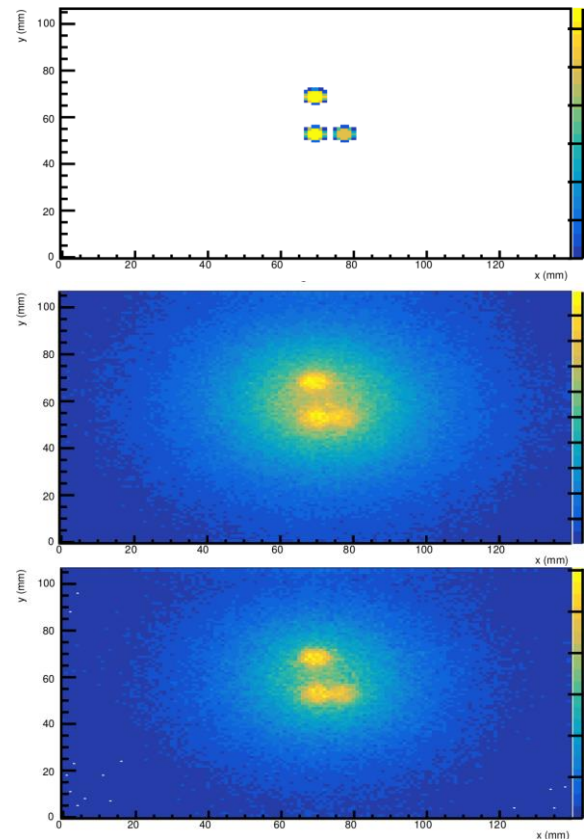


Fig. 3. Effects of hit energy and other cuts on reconstructed MC data; from top to bottom: Ground Truth phantom radioactive inserts; reconstructed image without cuts; 30 to 266 keV energy cut only and topological Compton mitigation dropping out events that present two distinct clusters of interaction in the scintillator.

A further equalization, generally finer, is performed on the acquired data, thanks to the fact that the charge collected by each anode is acquired separately and made available for image analysis and reconstruction.

Taking into account the MC simulation analysis for fine tuning of the optimal cuts in energy and cluster detection (for Compton scattering mitigation), Fig. 4 reports the reconstructed image of one of the acquired run of the two phantoms, where proper smearing is not applied to enhance the pixels structure of the detector system.

The simulations, in the aim of this work, is also used to estimate the activity of the sources starting from the insert counts extracted from the corresponding regions in the reconstructed images (as in Fig. 4): the counts on each region is the sum of the counts in the pixels which are totally or partially inside the circle of the region; counts in pixels shared by two regions are assigned to each region proportionally to the covered pixel area. The counts assigned to the insert are the counts of the corresponding region subtracted by the counts in the background region, scaled by their respective areas. The MC provides the fractions of photons emitted from one insert and detected in another region of the image; these fractions, reported in Table 1 for the same run of Fig. 4, are used to compute the expected activities in each insert from the measured raw counts.

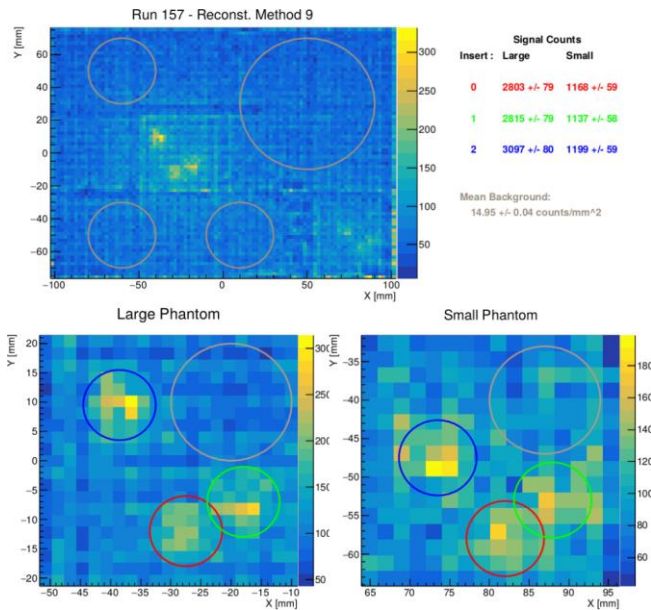


Fig. 4. Reconstructed image from real data (top); on the bottom part the zoom on the large (bottom-left) and small (bottom-right) phantoms with the 3 inserts filled with the beta-emitting  $^{90}\text{YCl}_2$ . The circles (masks) on the full image identify the regions used for the background evaluation, while in the zoomed images the smaller circles select the insert regions while the larger one the background. These areas are used to estimate the signal counts reported on top-right.

Fig. 5 shows the distribution of the preliminarily reconstructed activities (taking into account 4 ms dead time of the electronics) of the insert divided by the reference values extracted by the TDCR. These estimated activities, which are one of the main goal of the quantitative imaging, deviate on average from the “ground truth” by 3% (15% RMS) and 20% (6% RMS) for large and small inserts respectively.

TABLE I  
FRACTIONS OF GAMMA MIGRATIONS

Destination image region	Insert origin					
	Large phantom			Small phantom		
	0	1	2	0	1	2
0	64.48	21.63	13.39	61.84	24.56	15.34
1	22.08	66.28	11.02	22.53	61.55	13.75
2	11.85	10.47	73.83	14.56	12.9	69.76
Background	1.59	1.62	1.76	1.07	0.99	1.15

The fraction of photons emitted by each insert (columns) and reconstructed in the image regions (inserts and background, on rows) for the large and small phantoms.

#### IV. CONCLUSIONS

The above outlined approach, which tries to investigate and possibly mitigate the critical aspects of the quantitative bremsstrahlung radiation imaging, is still work in progress; the preliminarily experimental procedures using sub-optimized detectors for bremsstrahlung gammas and supported by Monte Carlo simulations analyses provide an estimated activity distribution of  $^{90}\text{Y}$  filled inserts within 30% from the reference values. In the current work, the choice of the gamma energy window combined to the assignment of the image pixels to the

different sources of radiation (insert and background), has represented the most critical, and still not fully solved question.

Analysis of the pin hole collimator data, better integration of MC and real data reconstruction, identification of the most effective function for figures of merit optimization, are underway and likely applied also to new data from  $^{166}\text{Ho}$  where some of the detector components have been optimized for gamma energy above 400 keV.

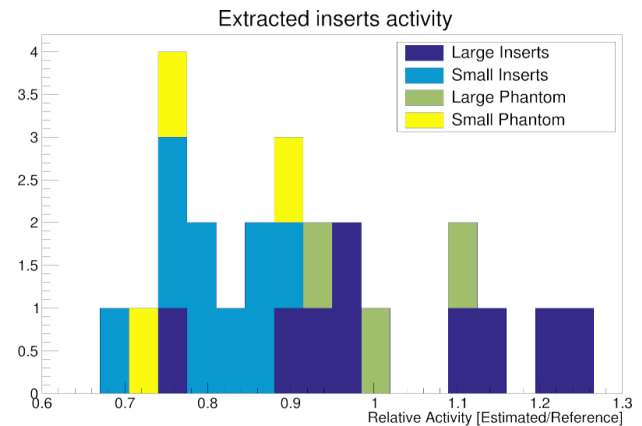


Fig. 5. The distribution of the estimated inserts activities over the reference values measured by the TDCR for three runs with different experimental configurations. Reported are also the total activity of each phantom respect to the reference.

#### REFERENCES

- [1] S. St James, et al., “Current Status of Radiopharmaceutical Therapy”. Int J Radiat Oncol Biol Phys. 2021 Mar 15;109(4):891-901, 10.1016/j.ijrobp.2020.08.035.
- [2] M. Capogni, P. De Felice, “A prototype of a portable TDCR system at ENEA”. Appl. Radiat. Isot. 93 (2014) 45-51, DOI: 10.1016/j.apradiso.2014.03.021
- [3] F. Garibaldi, et al. (2010), “A novel high resolution and high efficiency dual head detector for molecular breast imaging: New results from clinical trials.”, Nuclear Instruments and Methods in Physics Research Section A: Accelerators, Spectrometers, Detectors and Associated Equipment, 617(1):227–229. 11th Pisa Meeting on Advanced Detectors.
- [4] A. G. Argentieri et al., A Multichannel Compact Readout System for Single Photon Detection: Design and Performances Nucl. Instr. Meth. Phys. Res., 2010
- [5] OpenGate web page: <https://opengate.readthedocs.io/en/latest/> (last visited 04/08/2025)
- [6] Pandola, L., Andenna, C., and Caccia, B. (2015). Validation of the geant4 simulation of bremsstrahlung from thick targets below 3 mev. Nuclear Instruments and Methods in Physics Research Section B: Beam Interactions with Materials and Atoms, 350:41–48.